

Pamukkale Üniversitesi Mühendislik Bilimleri Dergisi





Production of nanofiber composite membrane from chitosan added polyamide-6/cellulose acetate (PA6/CA) and investigation of membrane permeability

Kitosan katkili poliamid-6/selüloz asetat (PA6/CA) nanofiber kompozit membran üretimi ve membran geçirgenliklerinin araştırılması

Abdullah Gül^{1*} , İsmail Tiyek²

 $^{1} Department \ of \ Materials \ and \ Energy, \ Hemp \ Research \ Institute, \ Yozgat \ Bozok \ University, \ Yozgat, \ T\"{u}rkiye. \\ abdullahgul 46@gmail.com$

²Department of Textile Engineering, Faculty of Engineering and Architecture, Kahramanmaras Sutçu Imam University, Kahramanmaras, Türkiye.

ismailtiyek@ksu.edu.tr

Ismantyck@ksu.cuu.u

Received/Geliş Tarihi: 03.12.2024 Revision/Düzeltme Tarihi: 27.01.2025 doi: 10.5505/pajes.2025.68338 Accepted/Kabul Tarihi: 11.02.2025 Research Article/Araştırma Makalesi

Abstract

PA6 nanofiber composite membranes are expected to be limited in their application area in the future, as they will be affected by environmental and sustainability policy sanctions due to their weak hydrophilic effects under high pressure and being hydrocarbon-based raw material. In this study, bio-based chitosan-doped PA6/CA composite nanofiber membrane surfaces were prepared using the electrospinning method. Nanofiber-structured composite membrane surfaces were prepared at different mixing ratios to improve the hydrophilic and permeability properties of the composite membranes, depending on the chitosan doping ratio. Membranes were characterized by SEM images, pore size, pore ratio, and contact angle measurements. Tensile and bursting strength and air permeability tests were performed to measure the mechanical properties of the membranes. The study was carried out using two types of water, pure and salt water, to determine the permeability and ion retention properties of the prepared membranes. The results showed that chitosan-doped PA6/CA composite structured nanofiber membrane surfaces played an important role in increasing the hydrophilicity. It was determined that depending on the chitosan additive ratio, the pore size decreased and accordingly the air permeability decreased. It was observed that there was a decrease in pure water permeability in parallel with the reduction in tensile and bursting strength. However, an increase in ion retention was observed in the study performed with salt water. All these results show that chitosan-doped PA6/CA nanofiber composite membranes can be very promising for microfiltration applications with their hydrophilic, mechanical, and permeability values.

Keywords: Elektrospinning, Nanofiber, Chitosan, Cellulose acetate, Polyamide 6, Membranes.

Öz

PA6 nanolif kompozit membranların yüksek basınç altında zayıf hidrofilik etkileri ve hidrokarbon bazlı hammadde olmaları nedeniyle çevre ve sürdürülebilirlik politikası yaptırımlarından etkilenecekleri için gelecekte uygulama alanlarının sınırlı olması beklenmektedir. Bu çalışmada, biyo bazlı kitosan katkılı PA6/CA kompozit nanofiber membran yüzeyleri, elektrospinning yöntemi kullanılarak hazırlandı. Kompozit membranların hidrofilik ve geçirgenlik özelliklerini geliştirmek amacıyla kitosan katkı oranına bağlı olarak farklı karışım oranlarında nanofiber yapılı kompozit membran yüzeyleri hazırlandı. Membranlar SEM görüntüleri, gözenek boyutu, gözenek oranı ve temas açısı ölçümleriyle karakterize edildi. Membranların mekanik özelliklerini ölçmek için çekme ve patlama mukavemeti ve hava geçirgenlik testleri yapılmıştır. Çalışma, hazırlanan membranların geçirgenlik ve iyon tutma özelliklerinin belirlenmesi amacıyla saf ve tuzlu su olmak üzere iki tip su kullanılarak gerçekleştirilmiştir. Sonuçlar, kitosan katkılı PA6/CA kompozit yapılı nanofiber membran yüzeylerinin hidrofilikliğin arttırılmasında önemli bir rol oynadığını gösterdi. Kitosan katkı oranına bağlı olarak gözenek boyutunun azaldığı ve buna bağlı olarak hava geçirgenliğinin azaldığı belirlenmiştir. Çekme ve patlama mukavemetindeki azalmaya paralel olarak saf su geçirgenliğinde de azalma olduğu gözlenmiştir. Ancak tuzlu su ile yapılan çalışmada iyon tutulumunda artış gözlenmiştir. Tüm bu sonuçlar kitosan katkılı PA6/CA nanofiber kompozit membranların hidrofilik, mekanik ve geçirgenlik değerleriyle mikrofiltrasyon uygulamaları için oldukça umut verici olabileceğini göstermektedir.

Anahtar kelimeler: Elektrospinning, Nanolif, Kitosan, Selüloz Asetat, Poliamid 6, Membran.

1 Introduction

Micro-filtration (MF) membrane technologies are used to separate impurities in fluids [1]. These types of membranes are highly required in wastewater application, water purifying, and concentration methods and are used in many application areas [2]. In MF technology, a contaminated liquid (water, etc.) is passed through a porous membrane with a nanofiber structure to separate impurities, particles, and suspended particles from the application process liquid. The most important feature that characterizes an absorbent membrane for MF treatments is the pore-diameter or pore-size [1]. The particle size that can

penetrate the media is mainly related to the pore-size, which affects the adequacy of the filter media, and fine fibers with low diameter provide the filter media with small pore-size, high density and filtering efficient [3]. Electrospun nanofibrous membranes may be a good candidate application area for MF with their nano-size fibers, small pore-sizes, light weight and effective permeability [4]. Additionally, this membrane technology offers unique features such as high surface area and high efficiency interconnectivity of pores [5].

Generally, nanofiber structure membranes obtained by the electrospinning method; Using advantages such as high porosity, and surface area and adjustable pore size, the

^{*}Corresponding author/Yazışılan Yazar

purification applications of multifunctional nanofibrous membranes for water are carried out with different approaches. One of these approaches is; that the nanofibrous surface is obtained from functional polymer material directly by electrospinning method; It is in the form of subsequent modification of the nanofiber membrane surface with functional polymer materials [6].

Different procedures are used to produce MF membranes, besides sol-gel, coating, phase inversion, and electrospinning methods [7]-[10]. Among these procedures, electrospinning is a simple and effective technique for fabricating polymerstructure membranes with high poro size, attractive surface properties, and exceptional permeability ratios [11]. The electrospinning method is a successful method that allows the production of mostly nano- or micro-sized fiber structures. The liquid solution (usually polymer solution) placed in a syringe is released into a high-electric area with aid of a power supply. The resulting electrical force tides over the surface tension of the liquid solution and creates a funnel (Taylor), allowing mostly nano-sized fibers to be obtained on the collector plate. Theoretically, the resulting fiber structure is endless. The pores on the membrane surface obtained in nanofiber structure by the electrospinning method are essentially formed by the entanglement of nanofibers and they are tightly connected to each other. These resulting membrane surfaces are capable of overcoming the low flow problem encountered in porous membranes owing to high porosity and wide surface areavolume rate [12]. With electrospinning technology, poly (vinylidene fluoride), polyvinyl alcohol, polyamide-6, polyethylene glycol, and polyacrylonitrile [13]- [17]. Nanostructured fibers can be produced by preparing different products, such as natural or synthetic polymers such as 2023 and cellulose acetate (CA) [18].

In many studies conducted with PA6, it has been stated that it exhibits good mechanical properties such as high breaking strength (12 ± 0.2 Mpa) and elongation at break (50-300%). With this characteristic structure, this polymer has attracted great attention in terms of its lifetime, especially in membrane applications. PA6 polymer has a wide usage area due to its low cost. It also has good mechanical properties such as bending strength, high tensile strength, and impact capacity. At the same time recyclable and resistant to mold and bacteria [19].

CA is considered the most important organic ester of cellulose, a polymer abundant in nature [20]. CA is widely used in many applications, including plastics, coatings, and fibers, due to advantages such as non-toxicity, transportation, and low cost compared to other polymers [21]. However, CA nanofibers can exhibit unique properties including biodegradability, thermal stability, and good chemical resistance [22].

Ch is a polysaccharide derivative obtained by deacetylation of chitin. Chitin is the second most common biopolymer in the world after cellulose. Chitin, the main component of shellfish such as crabs and shrimps, can also be found in the skeleton of insects and the structure of the cell walls of fungi [23]. Ch, one of the natural biopolymers, is a material that has attracted the attention of researchers for the last 50 years. Ch has many positive aspects compared to chitin; It has found use in many sectors such as food, cosmetics, agriculture, medicine, textile, and paper. It is effective in wound healing because it is nontoxic, biocompatible, and has antimicrobial performance properties. Recent research shows that it is widely used in high-performance filters, tissue engineering, biomaterials, and band-

aids [24]. It is quite difficult to obtain nanofibers from Ch by electrospinning due to its high viscosity. Therefore, it may be necessary to mix it with other materials that can adjust the viscosity value to optimum settings and help facilitate the process [25], [26].

The main aim of this study is to introduce an effective approach to the literature by expanding the use of bio-based sustainable resources such as Ch to obtain a functional MF membrane surface with good mechanical properties and a hydrophilic structure consisting of high-performance PA/CA composite nanofibers. This study is the first in the literature to study and evaluate functional nanofiber membrane surfaces in a composite structure with Ch doping on PA/CA mixture as matrix material. In this respect, it can serve to fill the gap in the literature. For the morphological characterization tests of the obtained nanostructured membrane functional surfaces, scanning electron microscopy (SEM), tensile and bursting strength, air permeability, contact angle, porosity ratio and size, permeability, and ion retention studies were carried out respectively. At the same time; by preparing a suitable solution for Ch-doped PA6/CA polymer mixtures, an electrospinning process that will allow the production of uniform and homogeneously distributed membranes has been successfully carried out. The resulting nanofiber diameters are approximately between 120-300 nm. When the mechanical properties of the obtained membrane samples were examined, it was seen that not only tensile strength but also burst strength test results showed similar results.

2 Material and method

2.1 Material

PA6 granular (Formula weight: 113.5 g/mol, density: 1.085 g/mL), acetic acid (CH₃COOH, 100%), formic acid (HCOOH, >98%), and cellulose acetate (CA) (C₁₂H₁₆O₈, Mn \sim 30.000 by GPC) were obtained from Merck. Chitosan (CAS No: 9012-76-4) was obtained from Acros Organics.

2.2 Method

To be used in nanofiber membrane production, solutions containing PA6, CA, and Ch at different concentrations were prepared, 20% solids content by weight. For this purpose, 7 different solutions were prepared by adding different ratios of Ch (0, 5, 10, 15, 20, 25, and 30%, by weighing in the total solids) to equal amounts of PA6/CA (50/50 by weight) (Table 1).

Table 1. Mixing ratios of Ch added in PA6/CA solution.

Code	Total solids content	PA6	CA	Ch
	(%)	(%)	(%)	(%)
0 Ch	20	50	50	0
5 Ch	20	47.5	47.5	5
10 Ch	20	45	45	10
15 Ch	20	42.5	42.5	15
20 Ch	20	40	40	20
25 Ch	20	37,5	37.5	25
30 Ch	20	35	35	30

Each solution was prepared as approximately 75 ml and mixed at 600 rpm. The solvent was a mixture of acetic acid and formic acid in a 50:50 consortium. The solution was first stirred at 50 °C for 30 minutes. Then, it was cooled to room temperature and stirred for 12 hours. Finally, it was processed in an ultrasonic mixer for 30 min at room temperature.

For nanofiber production, the semi-industrial multi-nozzle INOVENSO brand NanoSpinner PilotLine device (Figure 1) was used in the Materials Laboratory at Kahramanmaras Sutçu Imam University (KSU) USKIM.

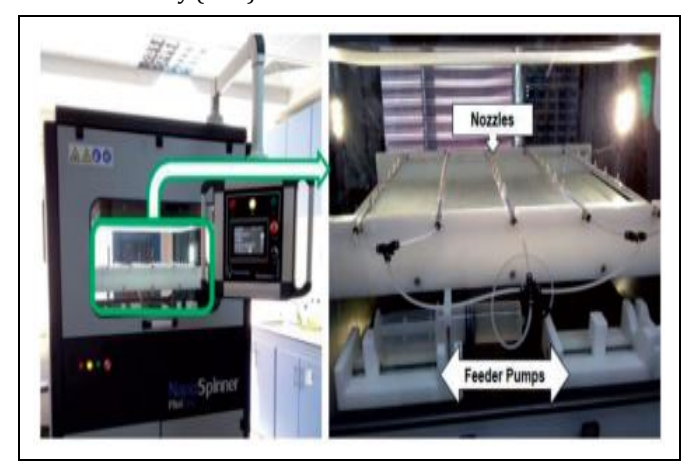


Figure 1. INOVENSO semi-industrial multi-nozzle electrospinning device.

All parameters that may affect fiber drawing during the process (such as power, feeding, needle tip-collector distance) were precisely adjusted with the preliminary trials conducted before. The values of the relevant parameters are given in Table 2.

Table 2. Electrospinning process parameters.

	Feed	Distance	Voltage	Total	Membrane	Fabric
	Rate	(mm)	(kV)	solid	ply	Winding
(mL/h)			ratio		Speed
				(%)		(cm/dk.)
0	0.4±0.1	195±2	29±1	20	50	10

The mixed solution was placed into the device using a 10 mL plastic syringe. White polypropylene spunbond nonwoven fabric with a weight of $12 \ (gr/m^2)$ and a width of 48 cm was preferred as the base material to ensure the accumulation of the produced fibers during spinning. The electrospinning parameters used in this study to obtain a smooth and continuous nanofiber membrane surface are given in Table 2.

2.2.1 Morphological analysis

The surface morphologies of the produced PA6/CA/Ch composite membranes were analyzed by SEM, ZEISS brand EVO/LS10 in KSU-ÜSKİM laboratories. To obtain higher resolution data from their analysis, the samples were coated with a thin layer of gold in a gold plating device (Cressington 108auto device) before SEM analysis. Magnifications of X1000, X5000, X10000, and X20000 were used for each sample. Additionally, 20 different fiber diameter measurements were made at X20000 magnification.

2.2.2 Mechanical Properties

Tensile strength, breaking elongation and Young's modulus of nanofiber-surfaced membrane samples were measured on the Zwick-Roell BT-1 device in the KSU-USKIM laboratory. Tensile tests of composite nanofiber membranes were accomplish corresponding to DIN EN ISO 2062 standard. Testing was done 3 times for each sample.

Bursting strength tests of composite membranes with an area of $20~\text{cm}^2$ samples were carried out according to the ISO 2758 standard. For each test sample, 5 test procedures were performed and their average values were taken into account.

Bursting resistance tests were performed on the Prowhite brand bursting test device located in the physical textile testing laboratory in KSU, Vocational School of Technical Sciences, Department of Textile Technologies.

2.2.3 Contact angle

KSV Attension brand Theta model contact angle measuring device was used to measure the contact angles of the produced membrane samples. The measurement technique used in this device is the method of dropping ultrapure water onto the membrane sample surface. Contact angle test measurements were carried out on the surface of dry membrane samples. As a method, at least 10 measurements were made for each membrane sample.

2.2.4 Pore size and porosity ratio

In this study, the average pore size (r_m) (Equation 1) was calculated with the filtration rate using the Guerout Elford-Ferry equation [27]-[29].

$$r_m = \sqrt{\frac{(2.9 - 1.75\varepsilon) \times 8\eta lQ}{\varepsilon A \Delta P}} \tag{1}$$

Here;

 ε : Membrane porosity ratio (%),

 η : Viscosity value of pure water (8.9 × 10⁻⁴),

l: Membrane thickness (*m*),

Q: Permeate volume per unit time

A: Effective area of the membrane

 ΔP : Applied bar (Mpa).

Additionally, in this study, the gravimetric method based on the weight of the liquid in the membrane pores was preferred to calculate the membrane porosity ratio (ε), which is the ratio of the pore volume of the membranes to the membrane geometric volume (Equation 2) [30]-[32].

$$\varepsilon (\%) = \frac{W_w - W_d}{A \times L \times \rho} \ 100 \tag{2}$$

Here:

 W_w : Wet weight of the membrane (g),

 W_d : Dry weight of the membrane (g),

A: Area of the sample (cm^2) ,

L: Average thickness of the sample (cm^2) ,

 ρ : Density of pure water (0.998 g/cm^3)

2.2.5 Water and air permeability

Performance tests of the membranes obtained by the electrospinning method against pure water and salt water were carried out. Pure water flux was measured using the aforementioned dead-end stirred cell filtration system. The membrane was pre-compacted at an applied pressure of 0.6 bar until a constant water flux was achieved. Water flux at a temperature of 25 °C was measured at the applied pressures of 0.6 bar. The equations below were used to calculate the hydraulic permeability for the membrane The features of the vacuum membrane filtration system used are given in Table 3 and the visual of the device is given in Figure 2.

Table 3. Technical information of vacuum filtration system.

Technical data	Technical value
Filter Membrane Area (m²)	0.00138
Maximum Filter Volume (mL)	250
Filter Vacuum Value (Bar)	0.6



Figure 2. Vacuum filtration device.

Performance tests of the membranes obtained by the electrospinning method were carried out by measuring the pure water and salty water (containing $NaNO_3$) permeability using a vacuum membrane filtration system. The features of the vacuum membrane filtration system used are given in Table 3 and the visual of the device is given in Figure 2.

The pressure filtration cell shown in Figure 2 was used to determine the pure water and $0.4\,\mathrm{M}\,\mathrm{NaNO_3}$ permeability values of the produced membranes. Before the permeability experiments, the produced membranes were soaked in pure water for 120 minutes at room temperature. The purpose of the wetting process is to prepare the membrane nanofibers for the process before the membrane flux process. After wetting, the flux at a pressure of 0.6 bar was calculated according to Equation 3. Permeability values were determined using the calculated flux value. Each sample was processed 10 times and average values were taken into account [27].

$$J_W = V / (A \times \Delta t) \tag{3}$$

Here:

 J_W is calculated as flux $(L/m^2 \times h)$, V is calculated as permeate volume (L), A is membrane active area (m^2) , and Δt is calculated as time (hour).

The permeability value is;

Permeabilite=
$$J/P$$
 ($L/m^2 \times h.bar$) (4)

It is obtained with the formula [27].

Air permeability testing of membrane samples was carried out on the PROWHITE Air Test-2 device located in the physical examination laboratory of KSU, Vocational School of Technical Sciences, Department of Textile Technologies. Test samples were prepared with an area of 20 cm² and were carried out at 100±10 Pa air pressure, taking into account the TS 391 EN ISO 9237 standard. For each test sample, 5 test procedures were performed and their average values were taken into account.

2.2.6 Ion retention

In the study, the ion retention performance of the produced membranes was analyzed using a pressure value of 0.6 bar and 0.4 M NaNO₃ salt solution. Salt permeability values of ionic salt

solutions at this pressure value were calculated using Equation 5. For salt removal rates, conductivity value measurements of the solutions with filtrate and feed were carried out in mV, and ion removal rates were stated as % using Equation 5 [30]. Three separate studies were conducted for each sample and the average value was taken into account.

$$R(\%) = \frac{C_f - C_p}{C_f} \tag{5}$$

In the formula; R refers to the ion retention (%), c_f refers to the electrical conductivity values of the feeding solution and c_p of the filtrate solution.

3 Results and discussions

3.1 Morphological analysis

SEM images of PA/CA composite electrospun nanofibers with different Ch doping ratios (0, 5, 10, 15, 20, 25, and 30%) are shared in Figure 3. The images obtained as a result of SEM studies showed that the fiber distribution and fiber diameters were uniform. The resulting fiber diameter plot (Figure 3) is shared.

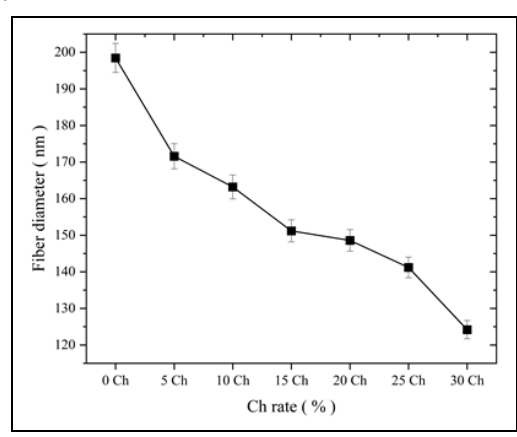


Figure 3. Diameter measurement graph of nanofibers obtained depending on Ch additive ratio.

When the morphology of the images of nanofibers taken from the SEM study is analyzed, it is understood that the fiber surface structures generally have a clear and distinct image. The SEM photo results given above prove that the morphology and average diameter of nanofibers can vary significantly depending on the Ch content in the prepared mixture. Additionally, the absence of bead structure in the images can be considered as evidence that the solution viscosity and electric field values are appropriate. However, it may be possible to encounter non-uniform fiber structures due to the increase in viscosity as the weight ratio of Ch increases [33], [34]. SEM analysis with a magnification of 20000 was applied to each of the samples without and with Ch added, and 20000 different measurements were made on the images and the average diameters were calculated (Figure 4). The resulting nanofiber diameters are approximately between 120-300 nm.

3.2 Mechanical properties

The castings obtained from the tensile tests performed on membrane samples with different Ch dopant and different Ch ratios are shared in Figure 5. The tensile force graph depending on the Ch doping ratio obtained from these strength graphs is shared in Figure 6.

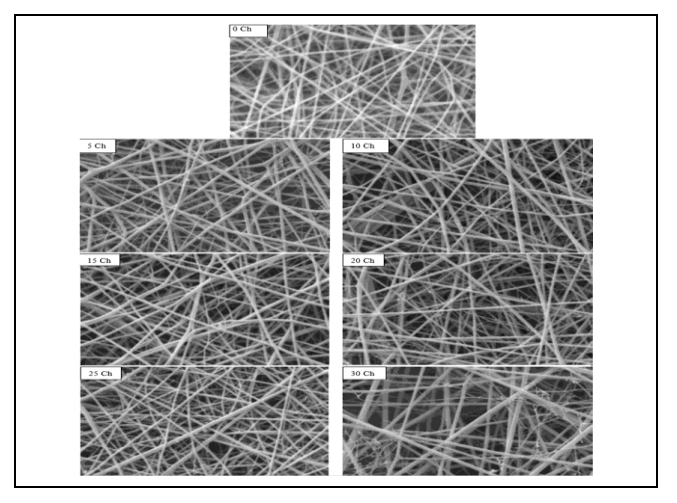


Figure 4. SEM images of nanofiber membranes obtained by electrospinning method.

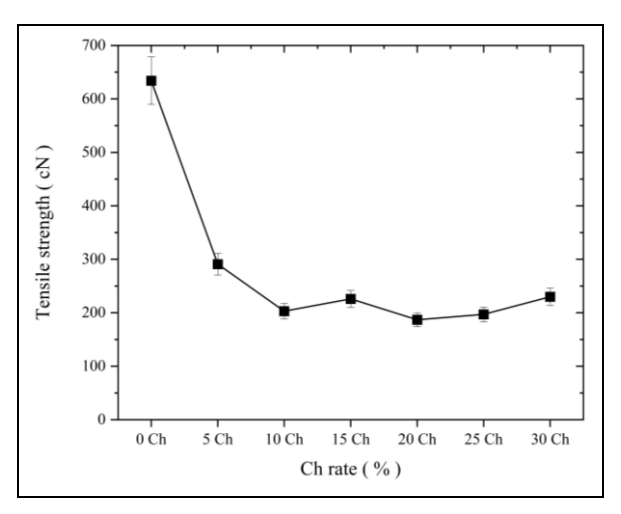


Figure 5. Tensile strength graph of nanofiber membranes depending on Ch doping ratios.

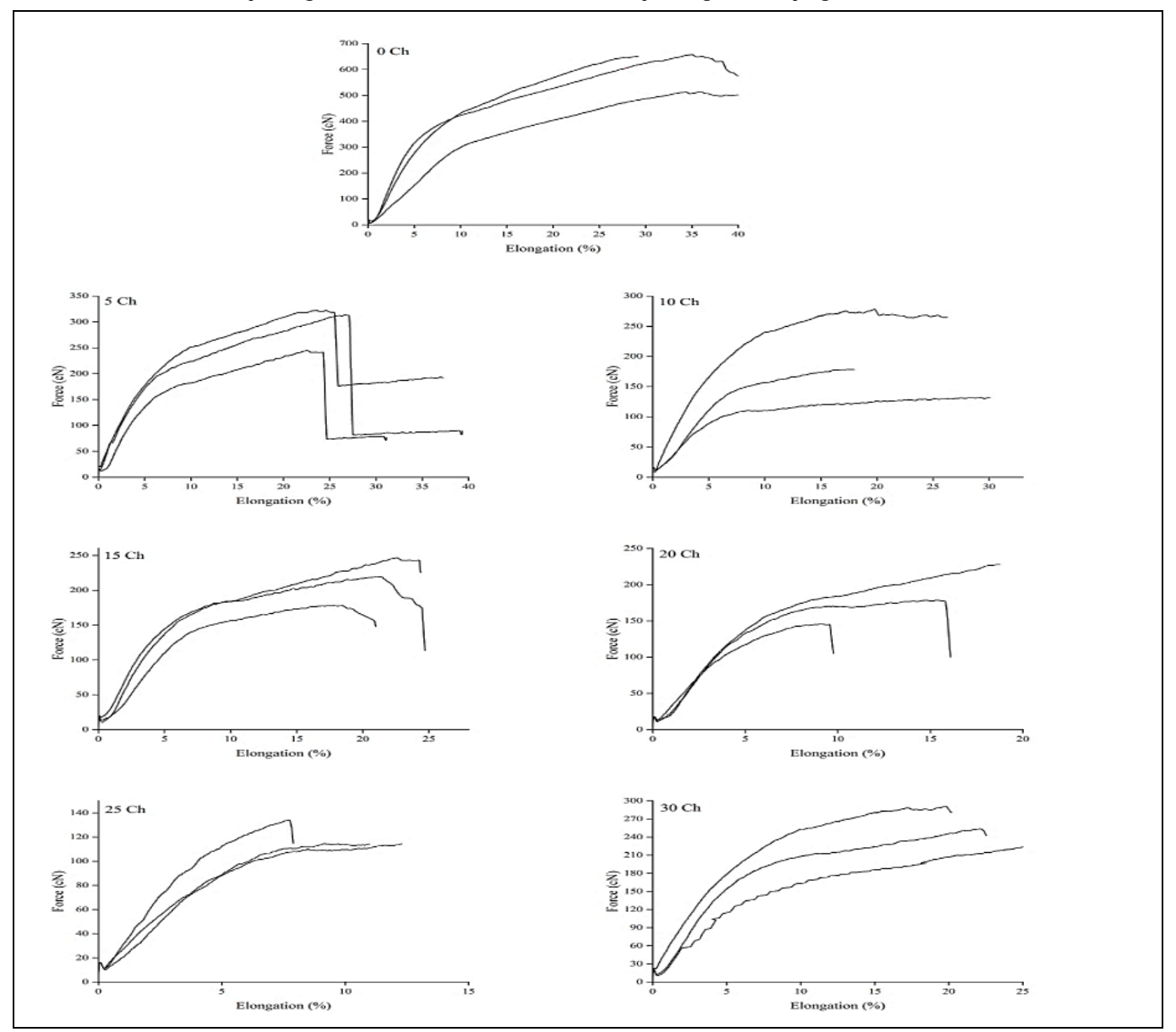


Figure 6. Strength graphs of nanofiber membranes produced depending on Ch doping ratios.

The strength values of nanofiber membranes without chitosan additives were found to be higher than the strength values of other Ch-doped nanofiber membranes. It was observed that after the 20% Ch sample, the tensile strength values started to increase as the weight percentage in the mixture increased. The decreasing tensile strength values with increasing Ch ratios can be explained by the weakening of the H bonds between the polyamide chains in the structure along with the increase of NH bands in the structure.

Additionally, the weakening in the bond structure can be explained by the increase in the stiffness structure [35]. In Chadded PA6/CA mixtures, as the Ch ratio increases, the hydrogen bonds in the structure are broken or weakened, and the formation of the amide plane in the -CO-N-H- plane can be observed with the energy and the added Ch ratio. With this study, it can be stated that new hydrogen bonds are formed between polyamide chains and Ch molecules after the mixing process [33].

The fact that Ch creates new hydrogen bond networks in the PA6 structure by changing its biological and mechanical properties is evidence that it creates an excellent bonding structure between polymers [36], [37]. Additionally, the Ch polymer chain structure contains amino and hydroxyl groups. It is a natural polymer that can provide hardness and brittleness properties in materials due to these groups in its structure [38].

The graph of the burst strength test results of nanofiber membranes obtained from PA6/CA polymers in the presence of increasing amounts of Ch is given in Figure 7.

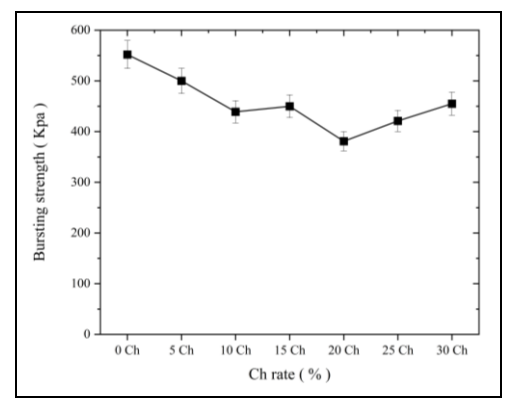


Figure 7. Burst strength graph of nanofiber membranes depending on Ch doping ratios.

As seen in Figure 7, as the Ch ratio increases up to 20%, the bursting strength value decreases. However, after this ratio, it is seen that the bursting strength value increases obviously. It is possible to say that the bursting strength increases depending on the membrane thickness and fiber diameter values, and these values show parallel results depending on the water permeability. This situation can be explained by the contribution of the change in the number of fibers per unit area and cross-section to the strength. As the membrane thickness increases, the cross-sectional area increases and the load carried by the cross-sectional area decreases. On the other hand, the number of obstacles encountered by water flux and permeability across the membrane increases. Water passes through the membrane more difficult. Therefore, permeability, which means the ease of passage of water through the

membrane, decreases. Air permeability and porosity results support these results.

3.3 Contact angle

Contact angle analysis was carried out to determine the hydrophobic (water escaping) and hydrophilic (water-loving) characters of the resulting membranes and is shared in Figure 8.

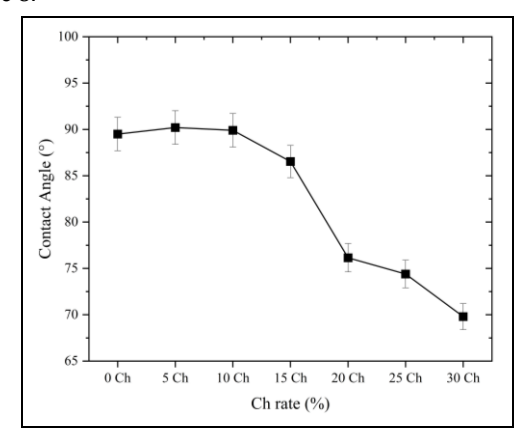


Figure 8. Contact angle graph of nanofiber membranes depending on Ch doping ratios.

The hydrophilic structure of the membrane material indicates that it has less resistance to the passage of water. In addition, the wettability of the surface prevents bacteria and organic substances from adhering to it and contributes to its ability to be washed more easily. It was stated in the study by Zhang et al. in the literature that Ch additive increases hydrophilicity. In the study of Ch-added membrane by Zhang et al., it was observed that the contact angle value decreased to 40-10° [33]. This information proves that Ch is a functional polymer.

Most importantly, water molecules bond to the hydrophilic membrane surface through hydrogen bonds, creating a thin water barrier between the membrane surface and the permeate solution. This serves as a boundary that prevents unwanted residues of hydrophobic membrane contaminants on the membrane surface [39].

3.4 Poro size and porosity ratio

Average pore size analyses calculated for the membranes using Equation 1 are shared in Figure 9. According to these results, as the weight ratio of Ch in the solution increased, the average pore size also decreased.

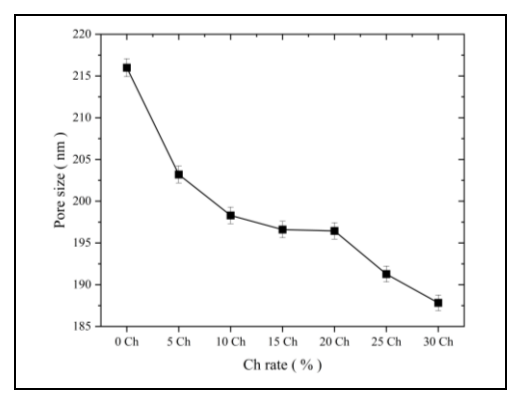


Figure 9. Pore size graph of nanofiber membranes depending on Ch doping ratios.

These results reveal that the average pore size decreases as the fiber diameter decreases, and can be defended as evidence that nanofibers contain high surface area. In addition, the results showed that membranes with larger fiber diameters have a larger porous structure between fibers. There are other studies in the literature that support this statement [40]. Porosity ratio test calculations for membranes obtained from Ch-doped PA6/CA mixtures were obtained according to Equation 2, and results are shared as percentage a Figure 10. As seen in the graph, as the amount of Ch in the membrane mixture increases, the porosity of the membrane structure decreases. However, the porosity value for all membrane modules was greater than 50%.

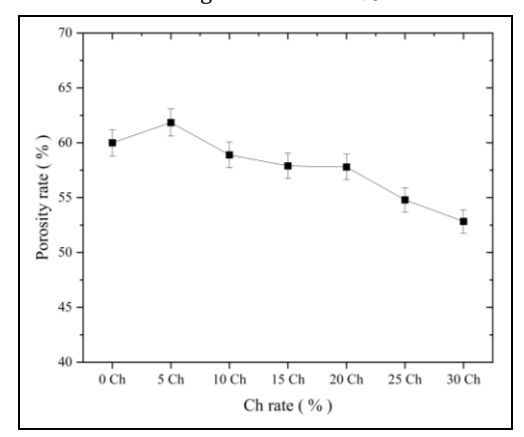


Figure 10. Porosity ratio graph of nanofiber membranes depending on Ch doping ratios.

3.5 Water and air permeability

In the permeability performance tests of Ch-doped PA6/CA nanofiber membranes obtained from Equations 3 and 4, the effect of two different flux values (water and saltwater) on the nanofiber membrane performance was evaluated. The study results regarding this are given in Table 4. When the results obtained were evaluated, it was observed that as the weight percentage of Ch increased, there was a decrease in the pure water and salt water flux values. In addition, the permeability value under 0.6 bar pressure decreases visibly. When the permeability values are examined, it is seen that the best pure water permeability value belongs to the 30 Ch sample.

In general, we see in literature studies that flux and permeability values are related to membrane nanofiber diameter and porous structure and are also proportional to membrane thickness values. In this context, it is generally observed that as the thickness of the membranes increases, the flux value also increases [41]. Chitosan, which contains very high amounts of amino and hydroxyl groups in its structure, can be used in wastewater treatment processes due to this feature [42]. As the fiber diameters decreased and the membrane

thickness decreased, the permeability value also decreased visibly.

Additionally, these results confirm that the flux decreases as the contact angle decreases. This confirms that the hydrophilic structure also gradually decreases. Rana and his colleagues argued that all three concepts are related to each other [43]. The increase in flux value as the Ch ratio in the solution concentration increases can be explained by the hydrophilic structure of Ch-doped membrane structures. The air permeability test results of nanofiber membranes obtained by adding Ch to the PA6/CA mixture, depending on the Ch mixture percentage, are shared in Figure 11. As the membrane thickness increases, the air permeability of the filter decreases [44]. The tested surfaces must be uniformly distributed nanofiber surfaces, and we can say that thin and thick areas have a significant impact on this performance.

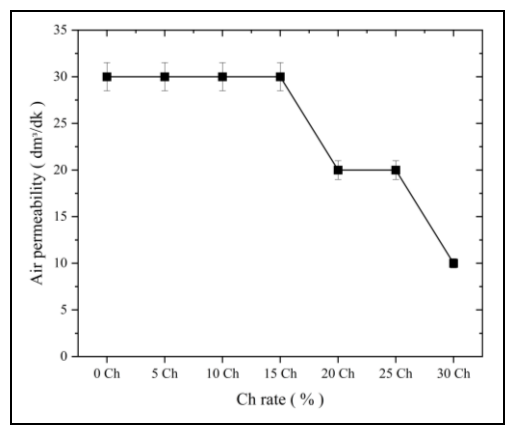


Figure 11. Air permeability graph of nanofiber membranes depending on Ch doping ratios.

The results obtained showed that with a certain increase in the Ch ratio, a certain decrease in air permeability levels was observed. We can say that this occurs due to the decrease in the diameter and porous structure of the fibers in the structure.

3.6 Ion retention

The ion retention graph obtained from the salt water mixture in the presence of 0.4 M NaNO3 of nanofiber membranes obtained from PA6/CA polymers in the presence of increasing amounts of Ch is given in Figure 12. According to these results, as the Ch ratio in the polymer solution generally increased, the ion retention percentage also increased. The presence of amine and hydroxyl groups in Ch causes the development of hydrogen and Van der Wall's bonds through PA6/CA mixtures. As these electrostatic interactions increase, cross-linking occurs which ensures the adhesion of salt ions [45]. Ch is used to clean metal ions and dye in water. As the weight percentage of Ch in the polymer mixture increases, the retention of salt ions in water also increases [46].

Table 4. Water and saltwater permeability and flux values of Ch doped membranes.

Ch ratio (%)	Water flux $(10^2 \times L/m^2 sa.)$	Water permeability $(10^2 \times L/m^2 sa. bar)$	Saltwater flux $(10^2 \times L/m^2 sa.)$	Saltwater permeability $(10^2 \times L/m^2 sa. bar)$
0 Ch	41±1	68±1	20±1	33±1
5 Ch	39±1	66±1	21±1	36±1
10 Ch	42±1	70±1	23±1	39±1
15 Ch	37±1	62±1	17±1	28±1
20 Ch	27±1	44±1	14±1	24±1
25 Ch	28±1	47±1	13±1	22±1
30 Ch	25±1	41±1	13±1	21±1

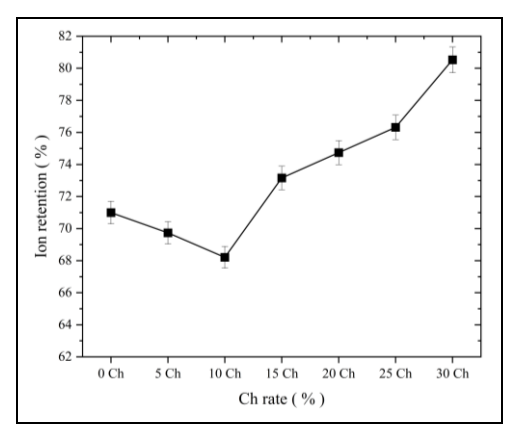


Figure 12. Ion retention graph of nanofiber membranes depending on Ch doping ratios.

4 Conclusions

As a general result; by preparing a suitable solution for Chdoped PA6/CA polymer mixtures, an electrospinning process that will allow the production of uniform and homogeneously distributed membranes has been successfully carried out. The resulting nanofiber diameters are approximately between 120-300 nm. As a result of the SEM studies, the images showed that the distribution of fibers and fiber diameters were uniform. When the mechanical properties of the obtained membrane samples were examined, it was seen that not only tensile strength but also burst strength test results showed similar results. PA6/CA membrane samples were subjected to contact angle testing separately, with and without Ch additives, and it was determined that as the Ch ratio of the membrane samples increased, the hydrophilic value also increased.

5 Acknowledgment

This study was supported by Kahramanmaras Sütçü İmam University BAP (Scientific Research Projects) unit with Project Number 2019/1-21D and the 100/2000 PhD scholarship awarded by YÖK (Council of Higher Education) in the field of smart materials.

6 Author contribution statements

In this study, Abdullah Gül worked on the production and experimental design of nanofibers. In addition, he took part in evaluating the test results and writing articles. İsmail Tiyek worked on the main idea of the project. However, the evaluation of the studies, general participated in the organization and interpretation of the manuscript.

7 Ethics committee approval and conflict of interest statement

"There is no need to obtain permission from the ethics committee for the article prepared". "There is no conflict of interest with any person / institution in the article prepared".

8 References

- [1] Baker RW. *Membrane Technology and Applications*. 4nd ed. California, USA, John Wiley, Sons Pres. 2012.
- [2] Gopal R, Kaur S, Ma Z, Chan C, Ramakrishna S, Matsuura T. "Electrospun nanofibrous filtration membrane". *Journal of Membrane Science*, 281(1-2), 581-586, (2009).

- [3] Hutten IM. Properties of Nonwoven Filter Media. 1st ed. Amsterdam, The Netherlands, Elsevier Publication, 2007.
- [4] Eichhorn SJ, Sampson WW. "Statistical geometry of pores and statistics of porous nanofibrous assemblies". *Journal of the Royal Society Interface*, 2(4), 309-318, 2005.
- [5] Focarete ML, Gualandi C, Ramakrishna S. Filtering Media by Electrospinning. Cham. 1st ed. Switzerland, Springer International Publishing 2018.
- [6] Li Y, Yuan D, Geng Q, Yang X, Wu H, Xie Y, Wang L, Ning X. "MOF-embedded bifunctional composite nanofiber membranes with a tunable hierarchical structure for highefficiency PM0.3 purification and oil/water separation". ACS Applied Materials & Interfaces, 13(1), 39831–39843, 2021.
- [7] Bentis A, Boukhriss A, Zahouily M, Manoun B, Gmouh S. "Functionalization of cotton fabrics by sol-gel method using ionic liquids with high-hydrophobic, excellent water repellent, oil/water separation, and self-cleaning properties". *Cellulose*, 30(10), 6719-6740, 2023.
- [8] Teng L, Yue C, Zhang G. "Epoxied SiO2 nanoparticles and polyethyleneimine (PEI) coated polyvinylidene fluoride (PVDF) membrane for improved oil water separation, anti-fouling, dye and heavy metal ions removal capabilities". *Journal of Colloid and Interface Science*, 630, 416-429, 2023.
- [9] Abuhasheesh YH, Hegab HM, Wadi VS, Al Marzooqi F, Banat F, Aljundi IH, Hasan SW. "Phase inverted hydrophobic polyethersulfone/iron oxide-oleylamine ultrafiltration membranes for efficient water-in-oil emulsion separation". Chemosphere, 337, 139431, 2023.
- [10] Naseeb N, Mohammed AA, Laoui T, Khan Z. "A novel PAN-GO-SiO2 hybrid membrane for separating oil and water from emulsified mixture". *Materials*, 12(2), 212, 2019.
- [11] Abushawish A, Bouaziz I, Almanassra IW, AL-Rajabi MM, Jaber L, Khalil AK, Chatla A. "Desalination pretreatment technologies: current status and future developments". *Water*, 15(8), 1572, 2023.
- [12] Akduman Ç. "PVDF electrospun nanofiber membranes for microfiltration: The effect of pore size and thickness on membrane performance". *European Journal of Science and Technology*, (16), 247-255, 2019.
- [13] Zhan B, Aliabadi M, Wang G, Chen ZB, Zhou WT, Stegmaier T, Ren L. "Underwater oleophobic electrospun membrane with spindle-knotted structured fibers for oil-in-water emulsion separation". *Langmuir*, 39(6), 2301-2311, 2023.
- [14] Yang Y, Zhou B, Yu L, Song G, Ge J, Du R. "Biosynthesis and characterization of antibacterial bacterial cellulose composite membrane composed of montmorillonite and exopolysaccharides". *International Journal of Biological Macromolecules*, 253, 127477, 2023.
- [15] Aygün HH. "Photochromic substance-doped PVA nanocomposite surface production and characterization: Determination of the appropriate polymer molecular weight for the electrospinning process". *Journal of the Faculty of Engineering & Architecture of Gazi University*, 40(1), 627-628, 2025.
- [16] Abd Halim NS, Mohd Hizam S, Wan Suhaimi, WMS, Ahmad Farid AS, Abd Rahman PNK, Wirzal MDH, Md Nordin NAH. "Nylon 6,6 waste nanofiber membrane for produced water filtration: experimental, performance modelling, optimization and techno-economic analysis". *Membranes*, 13(2), 224-242, 2023.

- [17] Cheng X, Li T, Yan L, Jiao Y, Zhang Y, Wang K, Shao L. "Biodegradable electrospinning superhydrophilic nanofiber membranes for ultrafast oil-water separation". *Science Advances*, 9(34), 1-9, 2023.
- [18] Karki HP, Kafle L, Ojha DP, Song JH, Kim HJ. "Cellulose/polyacrylonitrile electrospun composite fiber for effective separation of the surfactant-free oil-in-water mixture under a versatile condition". Separation and Purification Technology, 210, 913-919, 2019.
- [19] Li L, Bellan LM, Craighead HG, Frey MW. "Formation and properties of nylon-6 and nylon-6/montmorillonite composite nanofibers". *Polymer*, 47(17), 6208-6217, 2006.
- [20] Al-Rajabi MM, Haan TY. "Green extraction method of cellulose fibers from oil palm empty fruit bunches". *Journal of Kejuruter*, 34, 851-860, 2022.
- [21] Ju YW, Oh GY. "Behavior of toluene adsorption on activated carbon nanofibers prepared by electrospinning of a polyacrylonitrile-cellulose acetate blending solution". *Korean Journal of Chemical Engineering*, 34, 2731-2737, 2017, 2015.
- [22] Khalf A, Singarapu K, Madihally SV. "Cellulose acetate core-shell structured electrospun fiber: fabrication and characterization". *Cellulose*, 22, 1389-1400, 2015.
- [23] Özden D. Production of Chitosan Nanofibers Via Electrospinning for Filtration Applications, MSc Thesis, Erciyes University, Kayseri, Türkiye, 2011.
- [24] Gül A. A Research on Production of Nano-Structured Smart Membrane for Filter Applications. Doctoral Thesis, Kahramanmaraş Sütçü İmam University, Kahramanmaraş, Türkiye, 2022.
- [25] Ayodele O, Okoronkwo AE, Oluwasina OO, Abe TO. "Utilization of Blue Crab Shells for the Synthesis of Chitosan Nanoparticles and Their Characterization". Journal of Science and Technology, 40(5), 1043-1047, 2018.
- [26] Yunus H, Sabı EC, İçoğlu Hİ, Yıldırım B, Gülnaz O, Topalbekiroğlu M. "Characterization and antibacterial activity of electrospun polyethylene oxide/chitosan nanofibers". *Textile and Apparel*, 33(1), 1-8, 2023.
- [27] Islam MS, McCutcheon JR, Rahaman MS. "A high flux polyvinyl acetate-coated electrospun nylon 6/SiO2 composite microfiltration membrane for the separation of oil-in-water emulsion with improved antifouling performance". *Journal of Membrane Science*, 537, 297-309, 2017.
- [28] Li H, Shi W, Zhang Y, Zhou R, Zhang H. "Preparation of hydrophilic PVDF/PPTA blend membranes by in situ polycondensation and its application in the treatment of landfill leachate", Applied Surface Science, 346, 134-146, 2015.
- [29] Yin J, Zhou J. "Novel polyether sulfone hybrid ultrafiltration membrane prepared with SiO2-g-(PDMAEMA-co-PDMAPS) and its antifouling performances in oil-in-water emulsion application". *Desalination*, 365, 46-56, 2015.
- [30] Ghanbari M. Emadzadeh D, Lau WJ, Matsuura T, Ismail AF. "Synthesis and characterization of novel thin film nanocomposite reverse osmosis membranes with improved organic fouling properties for water desalination". *Royal Society of Chemistry Advances*, 5(27), 21268-21276, 2015.

- [31] Li RS, Liu B, Zhou M, Zhang ZX, Wang T, Lu BA, Xie EQ. "Effect of deposition voltage on the field emission properties of electrodeposited diamond-like carbon films". *Applied surface science*, 255(9), 4754-4757, 2009.
- [32] Liao C, Zhao J, Yu P, Tong H, Luo Y. "Synthesis and characterization of low content of different SiO2 materials composite poly (vinylidene fluoride) ultrafiltration membranes". *Desalination*, 285, 117-122, 2012.
- [33] Zhang H, Li S, White CJB, Ning X, Nie H, Zhu L. "Studies on electrospun nylon-6/chitosan complex nanofiber interactions". *Electrochimica Acta*, 54(24), 5739-5745, 2009.
- [34] Son WK, Youk JH, Lee TS, Park WH. "The effects of solution properties and polyelectrolyte on electrospinning of ultrafine poly (ethylene oxide) fibers polymer". *Polymer*, 45(9), 2959-2966, 2004.
- [35] Fu S, Yu Y, Wang F, Li J, Cai Z. "An antistatic agent based on polyionic liquid applied to nylon 6". *Green Chemical Engineering*, 5(3), 399-407, 2024.
- [36] Lin SJ, Hsiao WC, Jee SH, Yu HS, Tsai TF, Lai JY, Young TH. "Study on the effects of nylon-chitosan-blended membranes on the spheroid-forming activity of human melanocytes". *Biomaterials*, 27(29), 5079-5088, 2006.
- [37] Niu X, Qin M, Xu M, Zhao L, Wei Y, Hu Y, Huang D. "Coated electrospun polyamide-6/chitosan scaffold with hydroxyapatite for bone tissue engineering". *Biomedical Materials*, 16(2), 025014, 2021.
- [38] Zhou Q, Zhang J, Fang J, Li W, "The influence of nanofillers migration on the mechanical property of PA6/chitosan nanocomposites". *Royal Society of Chemistry Advances*, 5(22),16631-16639, 2015.
- [39] Xia S, Yao L, Zhao Y, Li N, Zheng Y. "Preparation of graphene oxide-modified polyamide thin film composite membranes with improved hydrophilicity for natural organic matter removal". *Chemical Engineering Journal*, 280, 720-727, 2015.
- [40] Hekmati AH, Khenoussi N, Nouali H, Patarin J, Drean JY. "Effect of nanofiber diameter on water absorption properties and pore size of polyamide-6 electrospun nanoweb". *Textile Research Journal*, 84(19), 2045-2055, 2014.
- [41] Acarer S. Multi-Scale Modeling of Manufactured Nanocomposite Membranes with Polymeric Matrix. Doctoral Thesis, Istanbul University, İstanbul, Türkiye 2020.
- [42] Ghani M, Gharehaghaji AA, Arami M, Takhtkuse N, Rezaei B. "Fabrication of Electrospun Polyamide-6/Chitosan Nanofibrous Membrane toward Anionic Dyes Removal". *Journal of Nanotechnology*, 2014(1), 278418, 2014.
- [43] Rana D, Matsuura T. "Surface modifications for antifouling membranes". *Chemical reviews*, 110(4), 2448-2471, 2010.
- [44] Dotti F, Varesano A, Montarsolo A, Aluigi A, Tonin C, Mazzuchetti G. "Electrospun porous mats for high efficiency filtration". *Journal of Industrial Textiles*, 37(1), 151-161, 2007.
- [45] Waheed S, Ahmad A, Khan S, -e-Gul S Jamil T, Islam A, Hussain T. "Synthesis, characterization, permeation and antibacterial properties of cellulose Acetate/Polyethylene, glycol membranes modified with chitosan". *Desalination*, 351(1), 59–69, 2014.

[46] Jabur A, Abbas L, Moosa S. "Fabrication of electrospun Chitosan/Nylon 6 nanofibrous membrane toward metal ions removal and antibacterial effect". *Advances in Materials Science and Engineering*, 2016(1), 5810216, 2016.